The role of lobes in chaotic mixing of miscible and immiscible impurities

T. H. Solomon*, S. Tomas and J. L. Warner
Department of Physics, Bucknell University, Lewisburg, PA 17837
(August 8, 1996)

Experiments compare long-range chaotic mixing of miscible and immiscible impurities in a time-periodic flow. For the miscible case, the transport is enhanced diffusion with an effective diffusion constant determined by lobes (turnstiles) that carry impurities between vortices. For the immiscible case, the impurity is broken into a distribution of droplets. If the characteristic droplet size is appreciably smaller than the lobe size, the transport is equivalent to that from the miscible case. Otherwise, interfacial tension results in reduction (and possibly extinction) of the transport.

47.52.+j, 66.10.-x, 51.20.+d, 92.10.Lq

The motion of a passive tracer in a two-dimensional fluid flow is known to be mathematically equivalent to the phase space trajectory of a Hamiltonian system [1,2]. If the velocity field is time-periodic, then the trajectories may be chaotic, showing sensitivity to initial conditions. When a miscible impurity is injected into such a flow, ordered and chaotic mixing regions form [3], characteristic of the phase space of a chaotic Hamiltonian system. This Hamiltonian formalism, however, is not rigorously valid for the mixing of an *immiscible* impurity (e.g., oil in water), since interfacial tension causes an attractive force between impurity particles, which therefore can no longer be considered to be following phase space trajectories. We describe here experiments that explore chaotic mixing of immiscible fluids, comparing the results to miscible mixing in the same flow. Despite the effects of interfacial tension, we demonstrate that the tools of chaotic advection can still be used to describe transport in the immiscible case.

Chaotic mixing of miscible impurities over distances larger than typical length scales of the flow ("long-range") can often be described as enhanced diffusion, where the variance of the concentration field grows linearly with time. It has been proposed [4] that the effective diffusion constant D^* for diffusive chaotic mixing (e.g., for time-periodic Rayleigh-Bénard convection [5]) can be explained theoretically by analyzing *lobes* [6] (or *turnstiles* [2]) that carry impurities between unit cells of the system. Our experiments verify these approaches by measuring independently the lobe areas and D^* for several miscible transport runs. Furthermore, we show that the lobes, which are Hamiltonian structures, provide the key to understanding mixing in the non-Hamiltonian, immiscible case.

The two-dimensional flow in these experiments is a chain of alternating vortices. This flow is chosen both for its simplicity and for its similarity to Rayleigh-Bénard (RB) convection. The flow is forced by a magnetohydrodynamic technique [7] (Fig. 1). A 10 mA current is passed through a 0.2 cm deep layer of salt water. This current interacts with an alternating magnetic field, produced by a linear array of Nd-Fe-Bo magnets below the fluid layer. This results in periodic forcing in the fluid, producing the alternating vortex structure (Fig. 1b). The side-walls of the inner cell employ a double-tab method [8] (Fig. 1c). The water interface curves upward slightly above the bottom ledge, but flattens out over the region of interest in the flow. This method allows floating oil droplets to explore the entire width of the flow field without sticking to the walls.

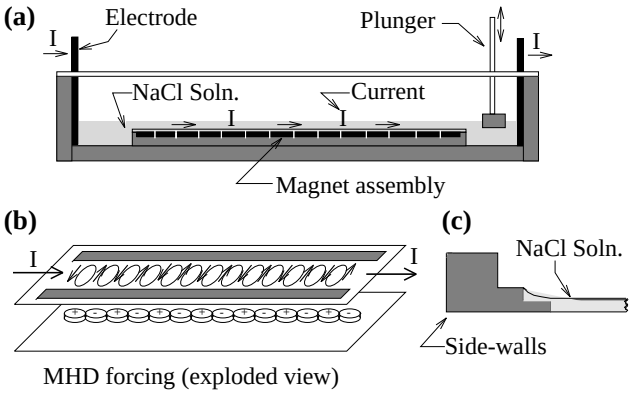

FIG. 1. Diagram of experimental apparatus. (a) Side view of apparatus. (b) Exploded view showing the magnetohydrodynamic forcing and a sketch of the chain of alternating vortices in the fluid layer above the magnet assembly. (c) Sketch of the side-walls and pinning of the fluid interface. The fluid layer trapped between the side-walls measures 3.8 cm x 26.7 cm, with a depth of 0.2 cm. The magnets each have a diameter of 1.91 cm.

For the "even" oscillatory instability of RB convection [9], a cross-section of the velocity field shows a chain of vortices that oscillate laterally. In our experiments, lateral oscillations are generated artificially by oscillating a small plunger vertically in the fluid (Fig. 1a), displacing the fluid *slowly* (no surface waves) back and forth across the (stationary) velocity field. Kinematically, the behavior is similar to that for the even oscillatory instability of RB convection, since the oscillation period for the plunger is 19 s, much longer than the viscous diffusion time

of 4 s. The magnitude of the time dependence is characterized by the dimensionless amplitude b = (oscillation amplitude)/(vortex width). While maintaining a realistic form for time dependence, this method has the advantage of allowing independent control of the oscillation amplitude and frequency, permitting much better quantitative measurements of transport than with RB convection.

For the miscible studies, uranine dye is mixed with a small amount of ethanol (to make the dye neutrally buoyant) and injected near the surface of the fluid layer in the central vortex. The fluid and dye are illuminated with fluorescent black light lamps and imaged from above with a CCD video camera.

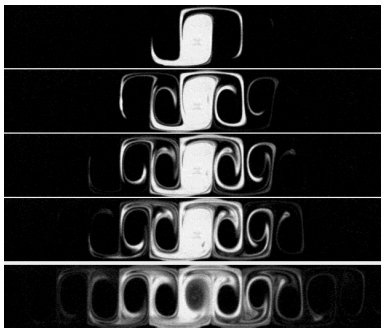

FIG. 2. Sequence of images showing the mixing of uranine dye; oscillation amplitude b=0.12. The images (starting from the top) are taken 18 s, 39 s, 57 s, 75 s and 189 s ($\approx$ 1, 2, 3, 4 and 10 oscillation periods) after the time dependence has been turned on.

Many of the classic signatures of chaotic mixing are apparent for the mixing of uranine dye (Fig. 2). Three lobes are apparent in the top frame of Fig. 2: two lobes carrying dye from the central vortex to its two immediate neighbors, and one lobe carrying clear fluid into the central vortex. The lobes are stretched by the flow and folded back repeatedly in the vicinity of the hyperbolic fixed points, similar to the stretching and folding typical of horseshoe and Bakers maps [10]. Kolmogorov-Arnold-Moser (KAM) invariant surfaces are manifested in these images as (temporary) barriers to fluid mixing, resulting in unmixed regions in the vortex centers. There are very slight secondary flows in the system due to Ekman pumping [11], shown by the hole in the central vortex that develops as initially clear fluid below the surface is circulated up through the center. This weak secondary flow, in conjunction with molecular diffusion, results in the eventual mixing of dye into the vortex centers.

A prediction for the effective diffusion constant D^* for this mixing process is obtained by measuring the area of the lobes. Assuming mixing within the vortices due to Ekman pumping, the ratio of the lobe area A_l to the vortex area A_v determines the flux F of impurity between vortices in one oscillation period. This flux is then inserted into a 1-D version of Fick's Law $F = D^* dc/dx$ (where c is the concentration), resulting in a prediction $D^* = (A_l d^2/A_v T)$ where $d = 1.91\ cm$ is the center-to-center vortex separation and $T = 19\ s$ is the period of oscillation. The results of this analysis are shown in Table 1 for experiments with amplitudes $b = 0.06, 0.12$ and 0.24.

An independent measurement of D^* is obtained by plotting the variance $\langle x^2 \rangle$ of the distribution as a function of time (Fig. 3) [12]. Scaling regions are apparent for oscillation amplitudes b=0.06 and 0.12, indicating diffusive mixing. D^* for the diffusive regime is one-half the slope of these plots. For b=0.06 and 0.12, the results (shown in Table 1) are $D^* = 0.007$ and 0.015 ($\pm$ 0.001) cm^2/s, respectively. These values agree with those from the lobe analysis, indicating that the simple lobe description of transport works very well. For the b=0.24 case, a clear scaling region can not be identified; however, the plotted slope from the lobe analysis is consistent with the growth of $\langle x^2 \rangle$ for intermediate times.

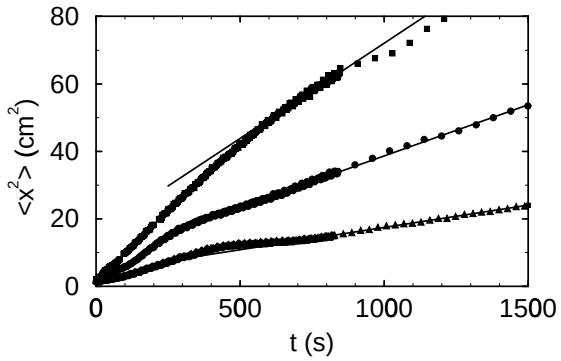

FIG. 3. Variance $\langle x^2 \rangle$ for mixing of dye; b=0.06 (triangles at bottom), b=0.12 (circles), b=0.24 (squares at top). Linear fits are shown as solid lines for b=0.06 and 0.12. For b=0.24, the solid line represents the lobe analysis prediction.

b ($\pm$ 0.01)	A_l (cm^2) ($\pm$ 0.04)	A_l/A_v ($\pm$ 0.006)	D^*_{lobe} (cm^2/s) ($\pm$ 0.001)	D^*_{var} (cm^2/s) ($\pm$ 0.001)
0.06	0.28	0.039	0.007	0.007
0.12	0.58	0.080	0.015	0.015
0.24	1.09	0.150	0.029	– – –

TABLE I. Determination of effective diffusion constant D^* for three oscillation amplitudes b. A_l is the lobe area, $A_v = 7.26\ cm$ is the vortex area, D^*_{lobe} is the result from the lobe analysis, and D^*_{var} is obtained from the variance measurements (see Fig. 3).

Experiments on immiscible mixing are conducted with a fluorescent oil (APD oil dye P/N 801) with viscosity 15 cp. The oil floats on the free surface of the water, so deformation of the flattened oil drops by the flow is affected by interfacial tensions between the oil and water and between the oil and air. In these experiments, the resiliency of the oil drops against deformation is characterized by the time τ for an elongated drop (from a recently-broken filament) with area 5 cm^2 to relax from an aspect ratio of 4 to 2 [13]. This resiliency is adjusted by varying the interfacial tensions with the addition of surface-active impurities (RBS cleaning solution) to the water. Three different conditions are studied: small, medium and large droplet resiliency with $\tau = 3$ s, 1.5 s, and 0.5 s, respectively.

The mixing of oil (Fig. 4) initially looks similar to that of dye (compare with Fig. 2). Oil crosses vortex boundaries in lobes near the hyperbolic fixed points and is stretched into thin filaments. Unlike a miscible impurity, however, filaments of oil are not stretched indefinitely; rather, the stretched filaments break, forming discrete droplets. The process continues until the oil has been broken down into a steady-state distribution of droplets [14]. (Previous studies have analyzed the steady state droplet distribution for breakup of oil due to chaotic advection [15].) If the oil's resiliency is large enough, the oil is not able even to cross between vortices (inset of Fig. 4); the oil is literally pulled back out of the lobes by the interfacial tension.

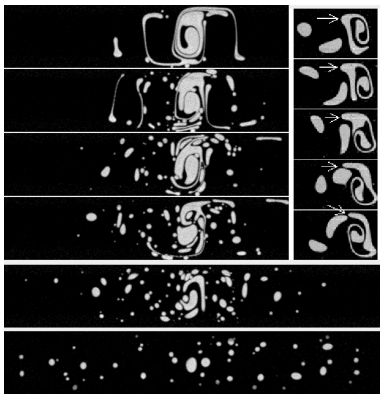

FIG. 4. Sequence showing the mixing of an immiscible impurity; oscillation amplitude b=0.12, small oil resiliency (τ = 3 s). The images (starting from the top) are taken 18 s, 39 s, 57 s, 75 s, 189 s, and 1890 s ($\approx$ 1, 2, 3, 4, 10 and 99 oscillation periods) after the time dependence has been turned on. The inset shows the corresponding process with larger resiliency (τ = 0.5 s); images are separated by 3 seconds each. In this case, interfacial tension prevents oil from being carried through the lobes (denoted by white arrows).

We analyze the immiscible transport problem using a simple phenomenological model in which steady-state droplet sizes are compared with the lobe size (measured for comparable miscible runs). We define a dimensionless droplet area $\Gamma \equiv A/A_l$, where A and A_l are the droplet and lobe areas. Conceptually, three regimes are expected, determined by the characteristic droplet scale Γ_c, defined such that half of the total amount of oil is contained in drops smaller than Γ_c. If $\Gamma_c \gg 1$ (*blob regime*), then the oil droplets are too large to be carried from one vortex to another through the lobes, resulting in no long-range transport. On the other hand, if $\Gamma_c \ll 1$ (*tracer regime*), then droplets are advected with the flow like (almost) passive tracers. In this regime, we expect the transport to be identical to that for the miscible case, since a miscible impurity is nothing more than a collection of small (molecular) tracer particles. The third *intermediate* regime is a cross-over regime between these two extremes.

The variance for the run shown in Fig. 4 is plotted in Fig. 5 (open squares) [16]. This plot has the same slope (within error) as that for a dye run with the same flow parameters (top solid curve in Fig. 5). The transport of oil therefore has the same D^* as for the miscible case, identifying this as a tracer regime run. A plot of the characteristic droplet area Γ_c for this run is shown in the inset of Fig. 5 (solid line). In the long time limit, $\Gamma_c \approx 0.17$, so the droplets are substantially smaller than the lobes, consistent with this being in the tracer regime.

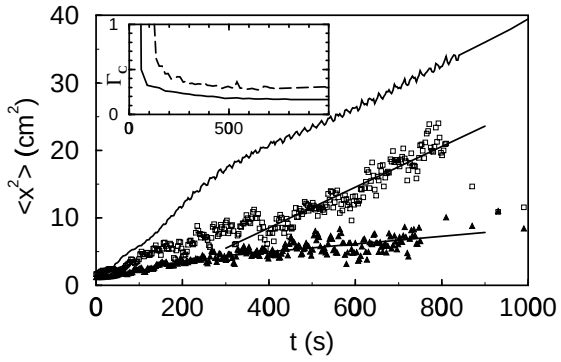

FIG. 5. Variance $\langle x^2 \rangle$ versus time for both oil and dye; b=0.12 in all cases; dye (top solid line), oil with τ = 3 s (open squares), oil with τ = 1.5 s (filled triangles). Linear fits are shown for the oil data, to be compared with the slope of the data for the dye. The inset shows the dimensionless characteristic droplet size Γ_c versus time (in s) for the same experimental runs; τ = 3 s (solid curve) and τ = 1.5 s (dashed curve).

In the immiscible transport run of Fig. 4, the two largest oil droplets remain in the central vortex [17]. The dimensionless area Γ of the second largest droplet (0.44), compared with that for the next largest droplet (0.30), indicates that there is an important cross-over scale $\Gamma \approx 0.3 - 0.4$. Specifically, drops with $\Gamma < 0.3$ participate in long-range transport, whereas drops with $\Gamma > 0.4$ do not. This cross-over scale is supported by another immiscible run with a larger droplet resiliency

(filled triangles in Fig. 5 and dashed line in the inset). The characteristic drop size Γ_c approaches 0.30 in the long-time limit, comparable to the cross-over length scale discussed above. The transport, in this case, is significantly smaller than for the run in Fig. 4, as would be expected if a substantial portion of the oil is not mixing. Assuming diffusive mixing, $D^* = 0.0028$ cm^2/s for this run, more than a factor of 5 smaller than the miscible result.

A mixing experiment with much higher resiliency (inset of Fig. 4) shows no transport at all: $D^* = 0$. (The data are not shown in Fig. 5.) There is some initial breakup of the oil into smaller droplets, but the drops remain larger than the lobe size, with $\Gamma_c \approx 2$ in the long time limit. The transport is almost completely halted after a short transient period [18]. This run is evidence of the *blob regime* discussed above.

Measurements have been made at other oscillation amplitudes b, and the results are consistent with those presented here. Experimentally, increasing b decreases the steady-state droplet areas while increasing A_l, dramatically lowering Γ_c and driving the system into the tracer regime. Conversely, the tracer regime is almost unattainable for smaller b. With an amplitude $b = 0.24$, Γ_c approaches 0.06 and 0.25 for $\tau = 3.0$ s and 0.5 s, respectively. In both of these cases, D^* is equivalent to that for the miscible case, within error. With $b = 0.06$, $\Gamma_c \approx 0.7$ for the smallest resiliency used ($\tau = 3.0$ s), and there is no long-range transport (blob regime). At this oscillation amplitude, the tracer regime is recovered only if the oil is broken up artificially, resulting in $\Gamma_c = 0.15$. In this case, the miscible result is recovered (tracer regime).

Summarizing, we have shown experimentally that the most significant features of long-range chaotic mixing can be interpreted by considering the lobes. For mixing of miscible impurities the lobe areas determine the effective diffusion constant D^*. The substantially more complicated immiscible problem can, as well, be understood by a remarkably simple model in which droplet sizes are compared with the lobe size. If the characteristic dimensionless droplet area $\Gamma_c \gtrsim 0.4$, there is no appreciable mixing. If $\Gamma_c \lesssim 0.3$, then the mixing is similar to that for the miscible case. If $0.3 \lesssim \Gamma_c \lesssim 0.4$, there is long-range mixing but with a reduced D^*. Experiments are currently in progress to study these problems with quasiperiodic and noisy time dependence.

We are pleased to acknowledge conversations with M. F. Schatz, who suggested the double-edge side-walls. Support for S. Tomas and J. L. Warner was provided by NSF REU through grant PHY-9423936. Equipment was provided by Research Corporation grant CC4002.

* Electronic mail: tsolomon@bucknell.edu

[1] H. Aref, J. Fluid Mech. **143**, 1 (1984).
[2] R. S. MacKay, J. D. Meiss, and I. C. Percival, Physica D **13**, 55 (1984).
[3] D. V. Khakhar, H. Rising, and J. M. Ottino, J. Fluid Mech. **172**, 419 (1986).
[4] R. Camassa and S. Wiggins, Phys. Rev. A **43**, 774 (1991).
[5] T. H. Solomon and J. P. Gollub, Phys. Rev. A **38**, 6280 (1988).
[6] V. Rom-Kedar and S. Wiggins, Physica D **51**, 248 (1991).
[7] H. Willaime, O. Cardoso, and P. Tabeling, Phys. Rev. E **48**, 288 (1993).
[8] M. F. Schatz, S. J. VanHook, W. D. McCormick, J. B. Swift, and H. L. Swinney, Phys. Rev. Lett. **75**, 1938 (1995).
[9] E. W. Bolton, F. H. Busse, and R. M. Clever, J. Fluid Mech. **164**, 469 (1986).
[10] T. M. Antonsen, Jr., A. Namenson, E. Ott, and J. C. Sommerer, Phys. Rev. Lett. **75**, 3438 (1995); J. M. Ottino, S. C. Jana, and V. S. Chakravarthy, Phys. Fluids **6**, 685 (1994).
[11] T. H. Solomon and J. P. Gollub, Phys. Fluids **31**, 1372 (1988).
[12] The variance is determined by fitting the smoothed concentration profile (obtained from the digitized image) to a Gaussian. This method reduces errors caused by dye leaving the visible portion of the cell.
[13] Tjahadi, Ottino and Stone (AIChE J. **40**, 385, 1994) have shown that this relaxation time is correlated with interfacial tension for suspended droplets. The problem for floating drops is currently being studied by P. DeRoussel and J. Ottino (private communication).
[14] The KAM barriers are ineffective in the immiscible transport experiments due to the finite extent of the droplets and to the weak Ekman pumping.
[15] F. J. Muzzio, M. Tjahjadi, and J. M. Ottino, Phys. Rev. Lett. **67**, 54 (1991); M. Tjahjadi and J. M. Ottino, J. Fluid Mech. **232**, 191 (1991).
[16] The variance data for the oil runs are more noisy than for the dye runs, since the variance is strongly dependent on the positions of individual drops of oil.
[17] In the calculation of the variance for this run, the two drops remaining in the center vortex are ignored by the Gaussian fits, so the variance calculations only account for the drops that participate in long-range transport.
[18] There is some long-range transport in these runs, due to tip streaming which generates some very small droplets that can be transported. These droplets, however, amount to less than 1% of the total oil in the system.